Chapter 22

Biosystems Control Design

Previous chapters have introduced the concepts of process dynamics and strategies for process control, emphasizing traditional applications from the petrochemical industries, such as chemical reactors and distillation columns. In this chapter, we introduce the application fields of bioprocessing and biomedical devices, and illustrate the characteristics that these processes share with traditional chemical processes. Differences will also be highlighted, including the nature of uncertainty in biological processes, as well as the safety considerations in medical closed-loop systems. Control system design for three bioprocessing operations is described: crystallization, fermentation, and granulation. Finally, a number of problems in controlled drug delivery are reviewed, and control strategies are demonstrated in the areas of diabetes and blood pressure regulation. Biological applications are expanded in Chapter 23, with a discussion of control systems opportunities, including applications to systems biology.

22.1 PROCESS MODELING AND CONTROL IN PHARMACEUTICAL OPERATIONS

A typical flowsheet in the pharmaceutical industry contains many of the same categories of operations as occur in a traditional petrochemical processing plant: reactors to generate products from raw materials, purification steps to extract desired products from the by-products and unreacted feed materials, and downstream processing associated with the final formulation of the product. Pharmaceutical processes are unique in several respects: (1) the main reactions involve biological materials, such as cells and tissues from more complex organisms, and (2) most of the products are formulated in solid form, which requires a unique set of bulk solids processing steps to purify and formulate the desired end product (e.g., a medicinal tablet). Consequently, the upstream processing involves sterilization and fermentation, and the manipulated inputs for the reactor often include "inducers" to activate the expression of particular genes in microbes in the reactor (gene expression is covered in more detail in Chapter 23). The downstream section of the flowsheet includes crystallization or chromatographic purification, to extract a high-purity product with desirable properties (e.g., chirality). Subsequent steps may involve solids handling and processing to produce final particulates with desirable properties, including dissolution attributes and tableting capability. These processes include mixing, classification, milling, grinding, crushing, granulation (agglomeration), tableting, and coating. Each of these operations has its own challenges and unique dynamic characteristics.

In the following sections, we consider three of the main processing steps in the pharmaceutical flowsheet: fermentation, crystallization, and granulation. Several of these processes appear in other industries as well (e.g., food, semiconductor, and specialty chemical), so the process control methods described find broad application in industry. It is important to note that the industry has a new emphasis on process systems engineering methods, driven by changes in FDA regulations (see PAT discussion in Chapter 18).

22.1.1 Bioreactors

Fermentation reactors are widely used in the pharmaceutical industries to make an array of important compounds, including penicillin, insulin, and human growth hormone. In recent years, genetic engineering has further expanded the portfolio of useful products that can be synthesized using fermentation methods (Buckland, 1984; Lim 1991; Schügerl, 2001). Despite the importance of this unit operation, the state of pharmaceutical fermentation operations is often characterized as more art than science, as with the winemaking industry (Fleet, 1993; Alford, 2006). Since 1990, there has been a focused effort to develop more sophisticated control architectures for fermentation operation, driven by the availability of new technologies for monitoring the quality of the contents of the fermentor (see, for example, Boudreau and McMillan, 2007).

A schematic of a fermentation process is given in Figure 22.1.

In a general sense, fermentation involves the generation of cell mass (product) from a substrate according to a simple reaction:

$$a\mathrm{C}_\alpha\mathrm{H}_\beta\mathrm{O}_\gamma + b\mathrm{O}_2 + c\mathrm{NH}_3 \rightarrow \mathrm{C}_\delta\mathrm{H}_\varepsilon\mathrm{O}_\zeta\mathrm{N}_\eta + d\mathrm{CO}_2 + e\mathrm{H}_2\mathrm{O} \tag{22-1}$$

where $\mathrm{C}_\alpha\mathrm{H}_\beta\mathrm{O}_\gamma$ is the substrate (reactant) and $\mathrm{C}_\delta\mathrm{H}_\varepsilon\mathrm{O}_\zeta\mathrm{N}_\eta$ is the cell mass (product). For example in beer making, the substrate is glucose (derived in the wort from grains), and the products are the alcohol and carbon dioxide gas, both of which contribute to the quality of the final product. This apparently straightforward reaction is complicated by the fact that it does not obey simple mass action kinetics; instead, the complex biochemistry underlying the reaction gives rise to unusual nonlinear rate expressions that characterize the enzymatic processes.

A simple dynamic model of a fed-batch bioreactor was given in Chapter 2, Eqs. 2-98 to 2-101. This model can be converted into mass balances on individual components as follows:

$$\frac{dX}{dt} = \mu(S)X - \frac{F}{V}X \tag{22-2}$$

$$\frac{dP}{dt} = Y_{P/X}\,\mu(S)X - \frac{F}{V}P \tag{22-3}$$

$$\frac{dS}{dt} = \frac{F}{V}(S_f - S) - \mu(S)X/Y_{X/S} \tag{22-4}$$

$$\frac{dV}{dt} = F \tag{22-5}$$

where the material balance in (22-2) details the conservation of biomass (X), Eq. 22-3 describes the production of metabolites by the cells (biomass), Eq. 22-4 details the conservation of substrate (S), and Eq. 22-5 is the overall material balance. The ratio F/V is often denoted as the dilution rate, D. The constants that appear in this equation include the feed concentration of the substrate (S_f), the yield of cell mass from substrate ($Y_{X/S}$), and the product yield coefficient ($Y_{P/X}$). The rate of the biochemical reaction, $\mu(S)$, typically utilizes Monod kinetics given by the saturating function:

$$\mu(S) = \frac{\mu_m S}{K_m + S} \tag{22-6}$$

where μ_m is the maximum specific growth rate (limiting value of the rate), and K_m is the substrate saturation constant. Control of this simple reactor involves

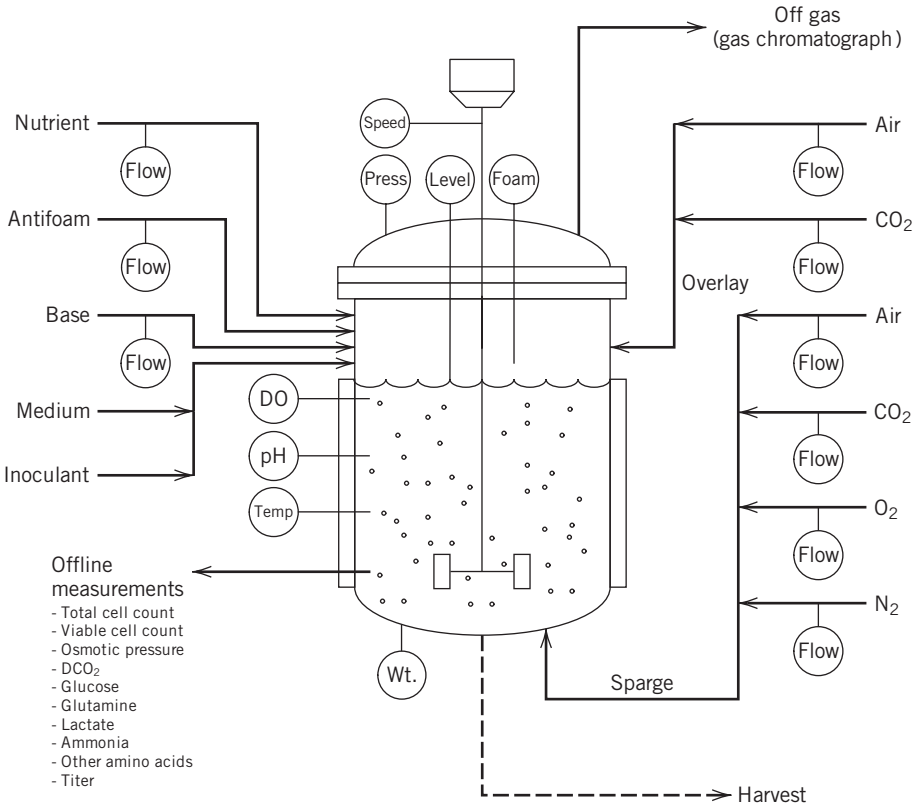

Figure 22.1 Schematic of a typical industrial fermentor. (Figure from Jon Gunther, PhD Thesis, Dept of Chemical Eng., UCSB, 2008).

manipulating the influx of substrate (via the dilution rate, D) to achieve an optimal level of production. More sophisticated control inputs are also possible, including inducers that stimulate the transcription of key genes in the microorganisms, leading to the synthesis of enzymes that maximize product yield.

One of the primary challenges to controlling these reactors in industry is the difficulty in measuring the status of the microorganisms in the fermentor. Specialized sensors (Mandenius, 1994) include enzyme electrodes (e.g., to measure glucose, lactate), calorimetric analyzers (e.g., to measure penicillin), and immunosensors (e.g., to measure antigens). However, it remains an open challenge to develop *in situ* sensors that can monitor a variety of metabolites within the microorganisms in real time.

EXAMPLE 22.1

Consider a fermentor, operated at constant volume, in which a single, rate-limiting substrate promotes biomass growth and product formation. Under the assumption of constant yield, one can derive the following material balances that describe the concentrations in the fermentor (Henson and Seborg, 1991):

$$\dot{X} = -DX + \mu(S, P)X \tag{22-7}$$

$$\dot{S} = D(S_f - S) - \frac{1}{Y_{X/S}}\mu(S, P)X \tag{22-8}$$

$$\dot{P} = -DP + [\alpha\mu(S, P) + \beta]X \tag{22-9}$$

For this reactor, the growth term has a more complex shape than the simple Monod expression presented earlier, because both substrate and product can inhibit growth:

$$\mu(S, P) = \frac{\mu_m\left(1 - \frac{P}{P_m}\right)S}{K_m + S + S^2/K_i} \tag{22-10}$$

The variables X, S, and P are the biomass, substrate, and product concentrations, respectively; D is the manipulated variable (dilution rate); S_f is the feed substrate concentration, and the remaining variables are fixed constants (yield parameters). Take the following values for the fixed parameters:

Table 22.1 Parameter values and units for fermentor in Example 22.1

$Y_{X/S}$	0.4 g/g	α	2.2 g/g
β	0.2 h^{-1}	μ_m	0.48 h^{-1}
P_m	50 g/L	K_m	1.2 g/L
K_i	22 g/L	S_f	20 g/L

(a) Assume a nominal operating point is $D = 0.202$ h^{-1} (dilution rate). The corresponding steady-state or equilibrium values of X, S, and P are [6.0 g/L; 5.0 g/L; 19.14 g/L]. Calculate the linearized model at this operating point, and determine the poles, zeros, and steady-state gain.

(b) Simulate the biomass X response to $\pm 10\%$ relative changes in dilution rate.

(c) Next, change the nominal dilution rate to $D = 0.0389$ h^{-1}. The corresponding equilibrium values of X, S, and P are [6.0 g/L; 5.0 g/L; 44.05 g/L]. (Does anything look unusual here?) Recalculate the linearized model at this operating point, as well as the poles, zeros, and steady-state gain.

(d) Simulate the biomass response to $\pm 10\%$ relative changes in dilution rate.

(e) Comment on the extreme differences in behavior of the fermentor at these two operating points. What does this indicate about this nonlinear system? What are the implications for control design?

SOLUTION

(a) Using the approach described in Section 3.3, a linearization of the nonlinear model (Eqs. 22-7 through 22-10) is performed. From the resulting model, one can derive a transfer function model with three poles and two zeros. The stable poles are calculated as the complex conjugate pair, -0.1469 ± 0.0694j, and the stable real pole at -0.2020. The zeros are both real and have the values: -0.1631, -0.2020. Finally, the steady-state process gain is -39.54.

(b) The simulated response is depicted in Fig. 22.2.

(c) As in part (a), the model is linearized, now at the new operating point. The poles are calculated as the complex

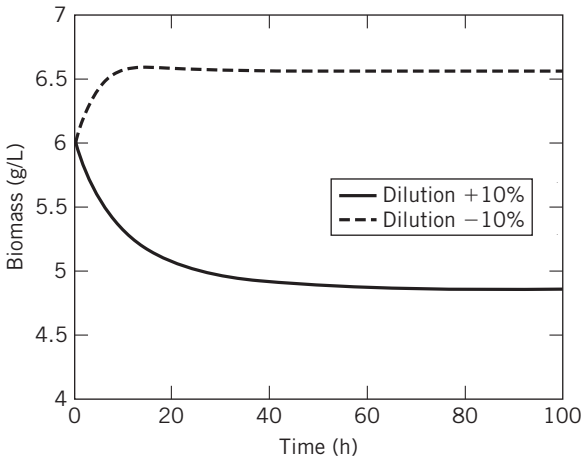

Figure 22.2 Step response of fermentor model to symmetric changes in D of magnitude 10% from the nominal value of $D = 0.202$ h^{-1}.

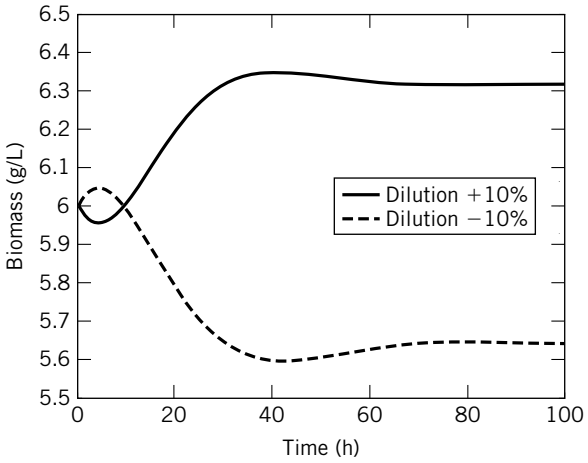

Figure 22.3 Step response of fermentor model to symmetric changes in dilution of magnitude 10% from the nominal value of $D = 0.0389\ h^{-1}$.

conjugate pair, $-0.0632 \pm 0.0852j$, and the stable real pole at -0.0389. The zeros are both real and have the values: 0.1630, -0.0389. Notice that one of the zeros is now nonminimum phase. Finally, the steady-state process gain is 86.90, indicating that the sign of the gain has been reversed.

(d) The simulated response is depicted in Fig. 22.3.

(e) In the first case ($D = 0.202\ h^{-1}$), the process gain was negative and the zeros were both negative. In the second case ($D = 0.0389\ h^{-1}$), the process gain was positive and one of the zeros becomes nonminimum phase, exhibiting inverse response. This suggests that the fermentor exhibits a dramatic nonlinearity, in which the gain can change sign and process zeros can change from negative to positive (indeed, a plot of the steady-state relationship between the dilution rate and the biomass for this fermentor reveals a parabolic shape; also see Exercise 2.15). This suggests that operation across this gain change requires a nonlinear controller or an adaptive control scheme.

22.1.2 Crystallizers

The operation of crystallization allows the separation of one phase (in this case, the solid from a solution mixture) so that the product has desirable properties. The solid product that results from crystallization is a highly ordered solid structure, which may have other desirable attributes, including morphology (e.g., shape), that are of direct benefit to the value of the final product. In the pharmaceutical industry, crystal size and shape may facilitate downstream solids processing and/or may be directly related to the final drug formulation, such as bioavailability, shelf life, toxicity, and drug dissolution (Fujiwara et al., 2005). Crystallization also finds application in the food industry to improve taste, as well as shelf life, for a diverse range of products (Larsen et al., 2006).

In order to explain the process control strategies employed in the operation of an industrial crystallizer, it is important to review briefly the concept of supersaturation and its relevance to crystallization (Larsen et al., 2006). Saturation refers to the property of phase equilibrium, in this case the equilibrium between the liquid and the dissolved solid (i.e., the solubility of the solid in the liquid). The state of supersaturation refers to the condition in which the liquid solution contains more solid than the amount that corresponds to the solubility (equilibrium), and the system exists in a so-called meta-stable state. Crystal formation can be induced by changing the operating conditions, such as temperature, so that the supersaturation state cannot be sustained, and a crystal is nucleated, or created, from the solution. As the dissolved component moves from the solution to the solid crystal phase, the concentration is, of course, lowered. Once a crystal is formed, it continues to grow as a function of the operating temperature and the concentration in the solution. In effect, the operation of crystallization involves the manipulation of this supersaturation state, trading off the formation of new crystals against the growth of existing ones.

An industrial crystallizer is operated typically in a batch mode, so that the management of the supersaturation state is accomplished over the course of the batch cycle time. The available manipulated inputs are the cooling jacket and steam flow rate, for temperature management, and the inflow of antisolvent (a component that lowers the solvation capability of the liquid) and solvent, to regulate the concentration of the solution (Zhou et al., 2006). A typical crystallization flowsheet is depicted in Fig. 22.4. Measurement of temperature is straightforward, and there are an increasing number of sophisticated instruments available for measurement of the crystal properties. These include turbidity sensors (to detect presence of solids), laser scattering instruments (to extract the distribution of crystal sizes in the unit), and spectroscopic instruments, e.g., attenuated total reflectance-Fourier transformed infrared (ATR-FTIR), for measuring solution concentrations (Fujiwara et al., 2005; Larsen et al., 2006). More recently, a variety of imaging techniques have been used to measure crystal-shape properties (morphology), such as width and length. As mentioned earlier, these size and shape properties are major determinants for the resulting utility of the product (e.g., drug solubility), and it may be desirable to produce crystals with very uniform properties (i.e., narrow size distribution).

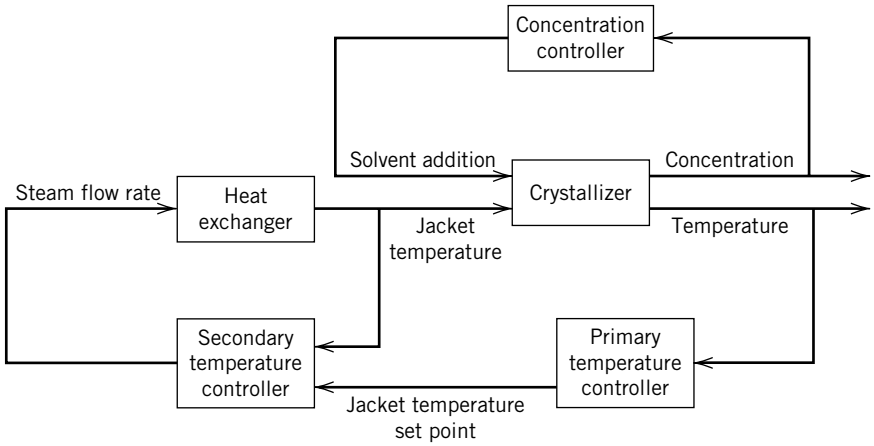

Figure 22.4 Flowsheet of a typical industrial batch crystallizer, showing concentration and temperature controllers, including cascade control for temperature.

22.1.3 Granulation

Granulation is a widely used process in which small particles agglomerate into larger granules. In wet granulation processes, the coagulation of particles is improved by the addition of a binder liquid, sprayed over an agitated powder in a tumbling drum or pan. The particles are wetted by the binder and a nucleate. The resulting binder-coated granules then collide and stick to form larger granules. These granules can also compact and consolidate as the binder liquid is brought to the surface of the aggregates by stirring in the granulator. Particles can also break because of collisions with the other particles or the granulator walls during mixing. Thus, the main phenomena in granulation processes are granule wetting and nucleation, consolidation and growth, and aggregation and breakage (Mort et al., 2001).

Granulation plays a key role in producing particles with special characteristics, such as time-release attributes (e.g., fertilizer, pharmaceutical tablet). However, in practice, inefficient operation, with very small yields and large recycle ratios (typically 4:1, recycle:product), often occurs. This inefficiency is due to the difficulty in designing and controlling granulation circuits that allow maintenance of specified size ranges for the granules.

As for crystallization, the key challenges for controlling a granulator are to produce particles with desirable attributes, to simplify downstream processing, and to realize end-product properties. In the pharmaceutical industry, granulation is usually accomplished in batch reactors, owing to the relatively small amount of material throughput. The key particle process that must be regulated is the agglomeration of smaller particles into larger particles. Manipulated inputs include binder spray addition (and/or viscosity), particle flow rate, recycle of oversize (crushed) and undersize (fines) particles, and changing the rate of agitation (mixing) in the vessel (Pottmann et al., 2000; Mort et al., 2001). Some applications also incorporate heating, which introduces temperature control considerations. The measurements currently available are the torque on the agitator (which yields an inference of the load in the vessel and its size and moisture content) and, in more recent installations, measurements of particle size (possibly as a distribution). When a particle distribution (PSD) is measured (e.g., by imaging methods or laser scattering), it is typically consolidated into one or more scalar measures of the distribution (e.g., the mean size, or d_x, the size of the particle in the xth percentile of the distribution (d_5, d_{90}, etc.)). A typical granulation flowsheet is depicted in Figure 22.5.

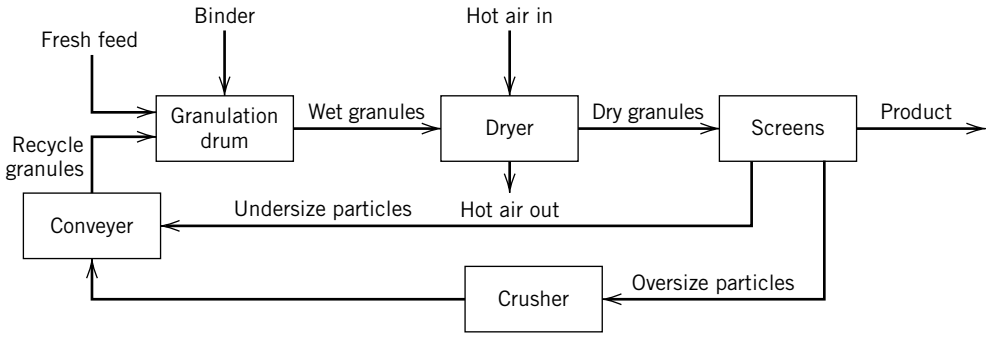

Figure 22.5 Process flowsheet for granulation circuit with recycle.

EXAMPLE 22.2

A simplified granulation flowsheet (Pottmann et al., 2000) is shown in Figure 22.6. The manipulated inputs are the liquid flow rates of binder introduced in three different nozzles, and the measured controlled variables are the bulk density and the 5th and 90th percentiles of the particle size distribution (d_5 and d_{90}, respectively). Pottmann et al. (2000) identified a first-order-plus time-delay model for each combination of inputs and outputs (3 × 3 problem) with the following parameters (time units are dimensionless):

$$G_{ij}(s) = \frac{K_{ij}}{\tau_{ij}s + 1} e^{-\theta_{ij}s} \tag{22-11}$$

$$K_{ij} = \begin{bmatrix} 0.20 & 0.58 & 0.35 \\ 0.25 & 1.10 & 1.30 \\ 0.30 & 0.70 & 1.20 \end{bmatrix} \tag{22-12}$$

$$\tau_{ij} = \begin{bmatrix} 2 & 2 & 2 \\ 3 & 3 & 3 \\ 4 & 4 & 4 \end{bmatrix} \tag{22-13}$$

$$\theta_{ij} = \begin{bmatrix} 3 & 3 & 3 \\ 3 & 3 & 3 \\ 3 & 3 & 3 \end{bmatrix} \tag{22-14}$$

The units for both the manipulated inputs and the measurements are dimensionless, and the nominal conditions (on which deviation variables are based) are: 180 for all three nozzles, 40 for bulk density, 400 for d_5, and 1600 for d_{90}.

(a) Using the relative gain array (RGA), determine the most effective pairings between the inputs and the outputs.

(b) Design three PI + Smith predictor controllers using the IMC design method (see Table 11.1, and assume that a value of $\tau_c = 5$ is employed). Keep in mind that the IMC/PI tuning is for the delay-free part of the plant with a Smith predictor.

(c) Simulate the system response for the three PI + Smith predictor controllers using a step set-point change of [10 0 0]. Be sure to enforce the constraints on the manipulated variables (lower bound of 105; upper bound of 345). Repeat the simulation for a step set-point change of [50 0 0].

SOLUTION

(a) The relative gain array is calculated as detailed in Section 16.2 from the process gains:

$$RGA = K \otimes (K^{-1})^T = \begin{bmatrix} 1.0256 & 0.6529 & -0.6785 \\ -1.4103 & 1.8574 & 0.5528 \\ 1.3846 & -1.5103 & 1.1257 \end{bmatrix} \tag{22-15}$$

Hence, the diagonal pairing of the controllers is recommended (1-1/2-2/3-3), because there are no negative values, and two of the three loops are paired on *RGA* values very close to 1.

(b) The individual controllers are given calculated from Table 11.1, row A:

Loop 1: $K_c = (2/5)/.2 = 2.0$; $\tau_I = 3$
Loop 2: $K_c = (3/5)/1.1 = 0.545$; $\tau_I = 4$
Loop 3: $K_c = (4/5)/1.2 = 0.667$; $\tau_I = 5$

(c) The simulation results are shown in Fig. 22.7 and 22.8. Note that enforcing the constraints for the second case leads to an unattainable set point for the first output.

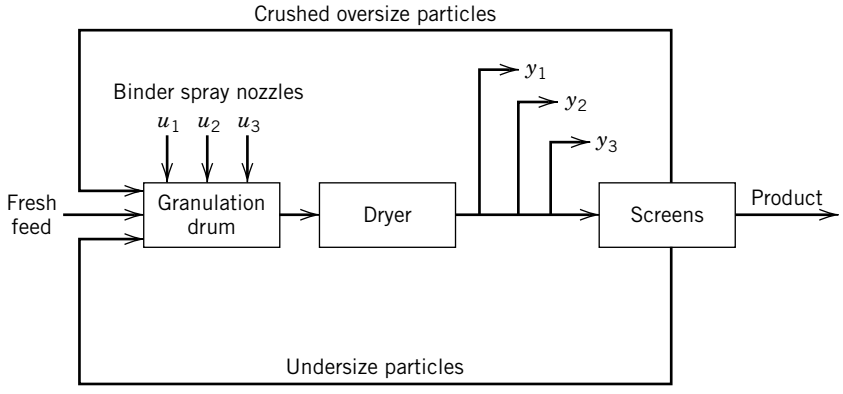

Figure 22.6 Simplified process flowsheet for granulator example. Here u_1, u_2, and u_3 are, respectively, nozzles 1, 2, and 3, and y_1, y_2, and y_3 are, respectively, bulk density, d_5, and d_{90}.

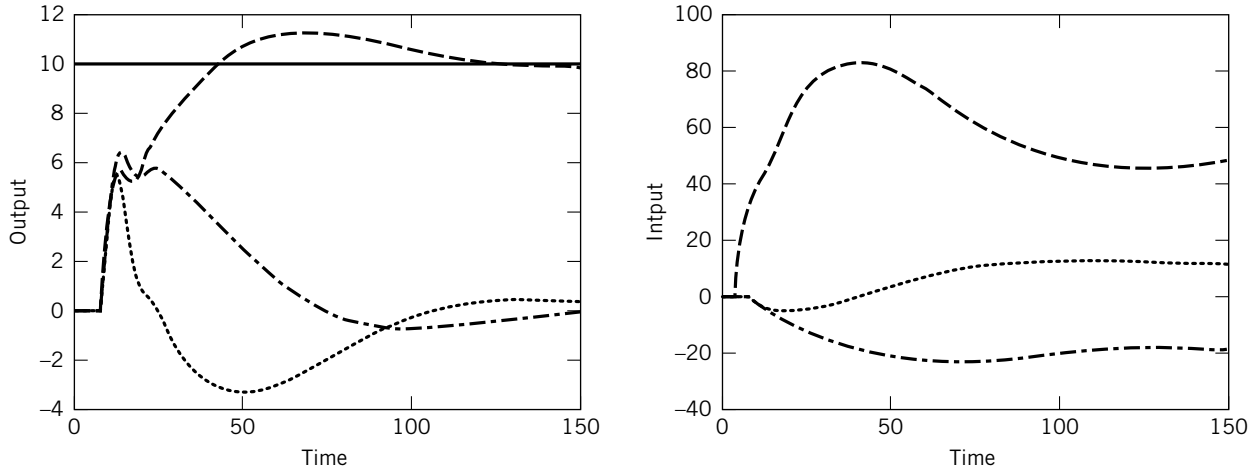

Figure 22.7 Closed-loop response of granulator to +10 step change in set point for y_1. left plot is CVs, right plot is MVs (----, y_1 and u_1; -.-.-.-., y_3 and u_3; ...., y_2 and u_2).

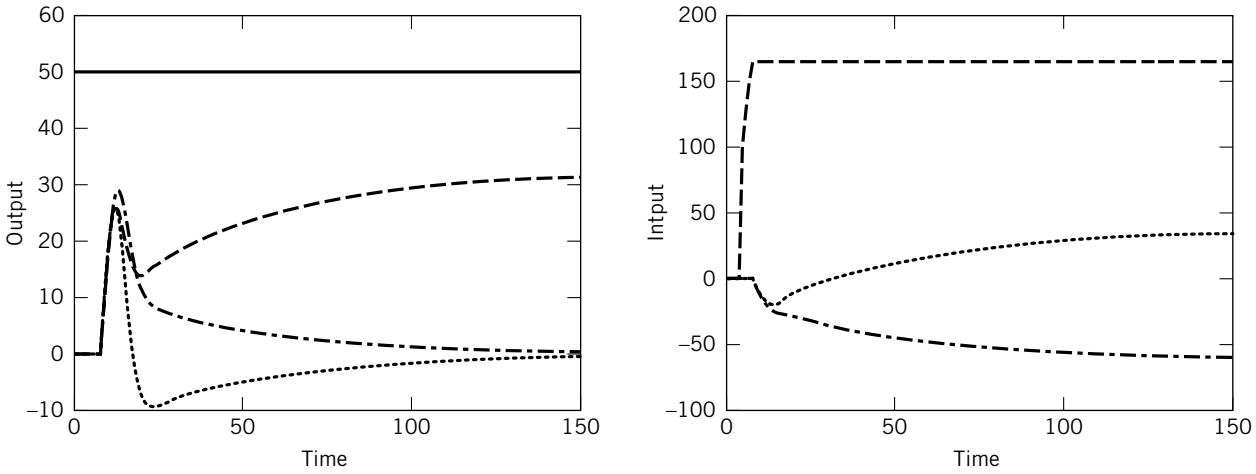

Figure 22.8 Closed-loop response of granulator to +50 step change in set point for y_1, with constraints enforced on the inputs. The left plot is CVs, right plot is MVs (----, y_1 and u_1; -.-.-.-., y_3 and u_3; ...., y_2 and u_2).

22.2 PROCESS MODELING AND CONTROL FOR DRUG DELIVERY

The human body is a remarkably complex biochemical process, and it shares many attributes with more traditional process control problems that have been discussed in earlier chapters. In the event that a body fails to achieve the robust level of self-regulation that occurs naturally (cf. Chapter 23), there are opportunities for medical intervention, often involving the administration of a therapeutic agent (or drug) in a prescribed manner. The therapy can be optimized using open-loop methods, but it is often advantageous to automate the process, thus removing the human from the feedback loop (much as a chemical plant removes the operator from the loop in the transition from manual control to automatic feedback control). In some medical applications (e.g., cancer treatment), control design can be used for decision support to guide medical interventions, and not strictly for automation. In the medical field, as in the process domain, there are three essential requirements for implementing feedback control: (1) the availability of a measurement that indicates the condition of the patient, (2) some knowledge of the underlying process dynamics (e.g., the effect of a drug on a patient's response), and (3) a suitable manipulated variable (e.g., drug or medication). Since 1990, there have been dramatic advances in sensor technology, as well as modeling and control strategies, for a variety of medical problems (see, for example, Hahn et al., 2002; Heller, 2005; Doyle et al., 2007).

In the following sections, a diverse range of biomedical applications that motivate the application of process control are described.

22.2.1 Type 1 Diabetes

In a healthy individual, the concentration of blood sugar (glucose), the body's primary energy source, is regulated primarily by the pancreas, using a combination of manipulated inputs that are analogous to the brake and gas pedal system used to control the speed of an automobile. As the blood sugar falls, the pancreas responds with the release of the hormone glucagon from the α-cells, which stimulates the breakdown of glycogen in the liver to create glucose, thus leading to an increase in glucose (i.e., the gas pedal). On the other hand, as blood glucose rises, the pancreatic β-cells release the hormone insulin that stimulates the uptake of glucose by muscle and fat tissue (Ashcroft and Ashcroft, 1992), and, consequently, the blood glucose level is decreased (i.e., the brake).

Type 1 diabetes mellitus is a disease characterized by failure of the pancreatic β-cells. In contrast, the primary manifestation of Type 2 diabetes is an inability, or resistance, of the cells to respond to insulin. The only treatment for Type 1 diabetes consists of exogenous insulin injections, traditionally administered in an open-loop manner by the patient. The insufficient secretion of insulin by the pancreas results in large excursions of blood glucose outside of the target range of approximately 80–120 mg/dL, leading to brief, or often sustained, periods of hyperglycemia (elevated glucose levels). Intensive insulin therapy can often have the unintended consequence of overdosing, which can then lead to hypoglycemia (low glucose levels). The consequences of such inadequate glucose regulation include an increased risk for retinopathy, nephropathy, and peripheral vascular disease (DCCT, 1993; Jovanovič, 2000; Zisser at al., 2005).

As illustrated in Fig. 22.9, a feedback controller can be used to regulate blood glucose using an insulin pump (widely available on the market today). There are preliminary clinical trials testing the efficacy of PID controllers for this delivery (Steil et al., 2006). The ADA has published guidelines (American Diabetes Association, 2006) recommending the following target zones for a blood sample drawn from a vein (a whole-blood sample):

- 80 mg/dL to 120 mg/dL before meals
- Less than 160 mg/dL 1 to 2 hours after meals

As indicated in Chapter 18, batch processes can benefit from recipe modifications in between consecutive batches or cycles, using a run-to-run (RtR) strategy. Run-to-run control strategies have also been developed for diabetes control, by considering glucose data for a meal response or an entire day to be the batch of interest. The similarities between the diabetic patient and the batch reactor recipe that motivate the application of this technique are the following:

1. The recipe (24-h cycle) for a human patient consists of a repeated meal protocol (typically three meals), with some variation on meal type, timing, and duration.
2. There is not an accurate dynamic model available to describe the detailed glucose response of each individual to the meal profile.
3. There are selected measurements available that might be used to characterize the quality of the glucose response for a 24-h day, including maximum and minimum glucose values.

Using currently available glucose meters, the blood sampling is very sparse, typically about 6–8 measurements per day; hence, the overall quality (i.e., glycemic regulation) has to be inferred from these infrequent samples. The results of a subsequent clinical trial (Zisser et al., 2005) demonstrated that a large fraction of the patients responded favorably to this type of control.

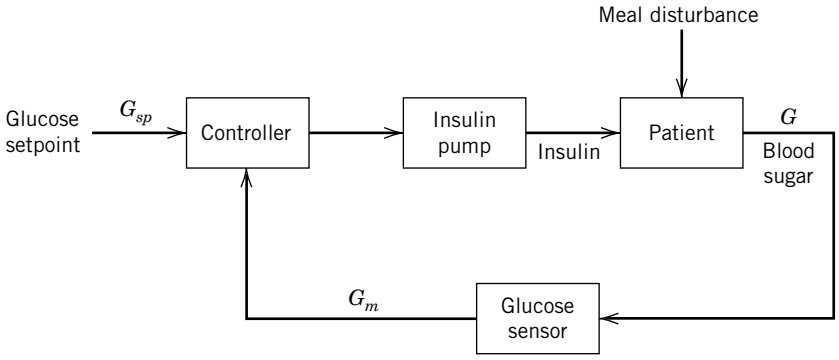

Figure 22.9 Block diagram for artificial β-cell, illustrating the meal as the most common disturbance. G denotes the blood sugar of the patient, G_m is the output of the glucose sensor, and G_{sp} is the glucose set point.

EXAMPLE 22.3

A patient with Type I diabetes needs an automated scheme to maintain her glucose within an acceptable range, widened here to allow less conservative control (54 mg/dL $< G <$ 144 mg/dL). She has just eaten a large meal (a disturbance) that you estimate will introduce glucose into her bloodstream according to $D(t) = 9.0\, e^{-0.05t}$, where t is in minutes and $D(t)$ is in mg/dL-min. She has a subcutaneous insulin pump that can release insulin up to 115 mU/min (mU = 10^{-3} Units of insulin). The "U" is a standard convention used to denote the strength of an insulin solution. The flow rate of insulin is the manipulated variable.

A simple model of her blood glucose level is given by Bequette (2002):

$$\frac{dG}{dt} = -p_1 G - X(G + G_{Basal}) + D \tag{22-16}$$

$$\frac{dX}{dt} = -p_2 X + p_3 I \tag{22-17}$$

$$\frac{dI}{dt} = -n(I + I_{Basal}) + \frac{U}{V_1} \tag{22-18}$$

where the constants are defined as follows: p_1 = 0.028735 [min^{-1}], p_2 = 0.028344 [min^{-1}], p_3 = 5.035E-5 [min^{-1}], V_1 = 12 [L], and n = .0926 [min^{-1}]. G, X, and I are values for glucose concentration (deviation) in the blood (mg/dL), insulin concentration (deviation) at the active site (mU/L), and blood insulin concentration, expressed in deviation variables. Basal values refer to the initial or baseline values for G and I (G_{basal} = 81 mg/dL and I_{basal} = 15 mU/L). D is the rate of glucose release into the blood (mg/dL-min) as the disturbance. U is the flow rate of insulin (mU/min) as the manipulated variable.

(a) What will happen to her blood glucose level if the pump is shut off initially?

(b) What will happen to her blood glucose level if the pump injects insulin at a constant rate of 15 mU/min?

(c) Is there a constant value of U that will help her stay within an acceptable glucose range (54 mg/dL $< G <$ 170 mg/dL) for the next 400 min?

SOLUTION

(a) As shown in Fig. 22.10, the patient's blood glucose will rise in a ramplike fashion if the insulin pump fails (i.e., shuts off). This can also occur as a result of a catheter occlusion (blockage) with the insulin pump.

(b) In this case (Fig. 22.11), the patient's blood sugar peaks, at slightly over 175 mg/dL, and takes 4 h to converge back to a steady-state glucose value of approximately 90 mg/dL.

(c) A setting of 25 mU/min yields the response in Fig. 22.12, which might be deemed too aggressive by many doctors, because of the low post-meal glucose values, motivating a more advanced (i.e., closed-loop) approach to glucose management.

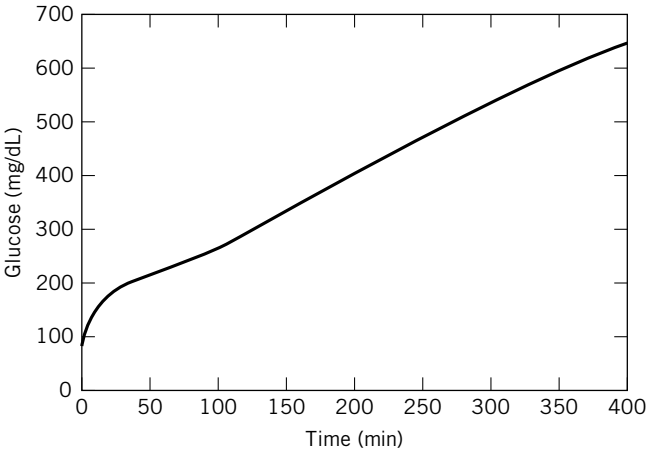

Figure 22.10 Open-loop response of patient's blood glucose when the insulin pump is turned off.

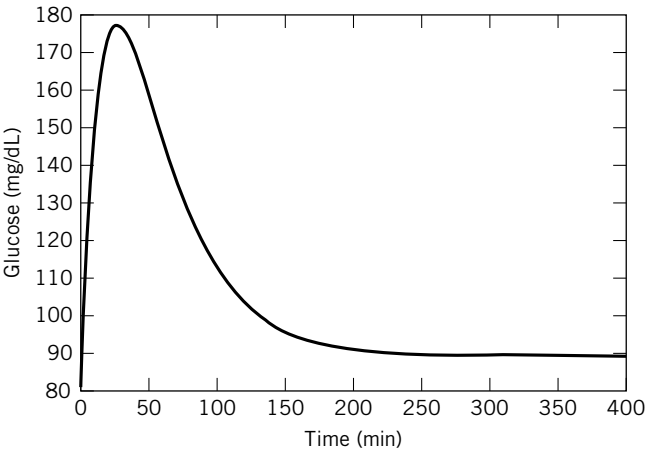

Figure 22.11 Open-loop response of the patient's blood glucose to a constant infusion rate of 15 mU/min from her insulin pump.

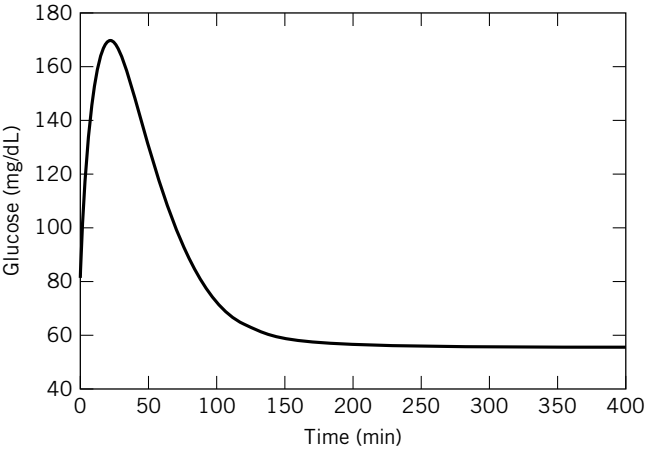

Figure 22.12 Open-loop response of patient's blood glucose to a constant infusion rate of 25 mU/min from her insulin pump.

22.2.2 Blood Pressure Regulation

In both the operating room and postoperative care contexts, closed-loop control of blood pressure and related variables (such as cardiac output and depth of anesthesia) have been studied for a number of years (e.g., Rao et al., 1999), and human clinical trials have proved the efficacy of the approach (Bailey and Haddad, 2005; Araki and Furutani, 2005). The postoperative application was handled typically by the administration of sodium nitroprusside (SNP) by a nurse via a continuous intravenous (IV) pump. SNP is a vasodilator that achieves blood pressure reduction by relaxing the muscles controlling the vascular resistance to flow through blood vessels. The current technology for both sensors and infusion pumps is facilitating the design of completely automated control strategies.

The context of the operating room is more complicated, with many critical variables that must be monitored. But an advantage of this setting is that nonportable sensors can be employed that would be too cumbersome or impractical for ambulatory applications. The measured variables include mean arterial pressure (MAP), cardiac output (CO), and depth of anesthesia (DOA). The DOA has been the subject of intense research activity over the last decade, and sensors are available to determine the depth of anesthesia through correlations. These sensors are inferential (see Chapter 15), in that they do not directly measure the medical state of anesthesia, which is characterized by such patient responses as hypnosis, amnesia, analgesia, and muscle relaxation (Araki and Furutani, 2005); rather, they measure the state of electrical activity in the patient's brain. One of the more promising methods is the bispectral index, derived from signal analysis of an electroencephalograph (EEG) (Bailey and Haddad, 2005). A variety of manipulated inputs are also available, resulting in an intrinsically multivariable control problem. Some candidate manipulated variables include vasoactive drugs, such as dopamine and SNP, as well as anesthetics (isoflurane, propofol, etc.).

EXAMPLE 22.4

Consider the following model for predicting the influence of two drugs: SNP, [μg/kg-min]) and dopamine (DPM, [μg/kg-min]), on two medical variables (MAP, [mmHg]) and CO, [L/(kg-min)]), where time is measured in minutes (Bequette, 2007):

$$\begin{bmatrix} MAP \\ CO \end{bmatrix} = \begin{bmatrix} \dfrac{-6e^{-0.75s}}{0.67s+1} & \dfrac{3e^{-s}}{2.0s+1} \\ \dfrac{12e^{-0.75s}}{0.67s+1} & \dfrac{5e^{-s}}{5.0s+1} \end{bmatrix} \begin{bmatrix} SNP \\ DPM \end{bmatrix} \qquad (22\text{-}19)$$

(a) Calculate the RGA for this problem and propose the appropriate control-loop pairing.

(b) Consider the pairing, SNP-MAP and DPM-CO, as is typically used in practice. Design a pair of PI controllers for this process, using the IMC tuning rules (Table 11.1) and choosing a value of τ_c for each controller that is equal to the corresponding open-loop time constant for that subsystem.

(c) Simulate the closed-loop response to a –10 mmHg change in the MAP set point, while holding CO constant. Discuss the extent of control-loop interactions.

SOLUTION

(a) Using the RGA calculation in Eq. 16-34, $\lambda_{11} = 0.4545$; therefore, the loop pairings apparently should be the 1-2/2-1 pairing, SNP-CO and DPM-MAP.

(b) From Table 11.1, the following values for the PI controller settings are calculated:

Loop 1: $K_c = -(0.67)/(6*(0.67 + .75)) = -0.0786$

$\tau_I = 0.67$

Loop 2: $K_c = (5)/(5*(5 + 1)) = 0.1667$

$\tau_I = 5$

(c) The simulated response for the MAP set-point change is depicted in Fig. 22.13, where there is a modest undershoot in the MAP response; however, the interacting nature of the process leads to a large excursion in CO. The control tuning (τ_c) could be refined to trade-off speed versus overshoot and interaction, or by designing a multivariable controller, such as MPC.

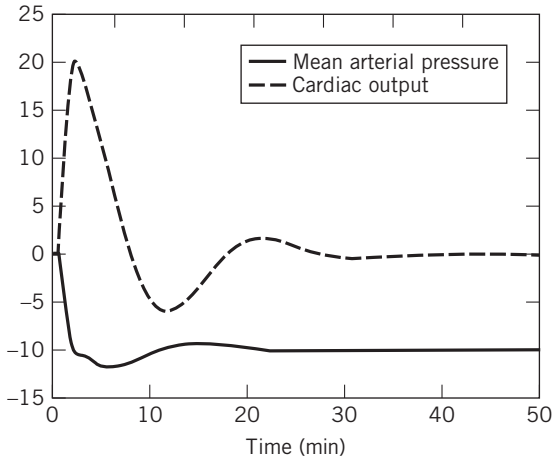

Figure 22.13 Closed-loop response of patient's mean arterial blood pressure and cardiac output to a –10 mmHg change in the MAP set point.

22.2.3 Cancer Treatment

Cancer treatment has changed dramatically over the past decade, in large part enabled by advances in imaging technology. Surgery has been the classical method for attacking cancerous tumors, and more recently

X-ray radiation has been employed. An unfortunate side effect in both cases is that healthy tissue can be compromised by inappropriate surgery or delivery of radiation, respectively. Chemotherapy is often used, alone or in conjunction with surgery or X-ray treatment, and has the advantage that undetected metastases (cancer cells that have circulated through the bloodstream) can be attacked with this method. Thermal therapies (radio frequency, microwave, or laser techniques) have also been demonstrated to be effective, with similar requirements on targeting the energy to the localized region of the tumor (Dodd et al., 2000). In thermal and radiation treatment, feedback control is finding application to the optimized delivery of the treatment (radiation, heat) to the targeted area (Salomir et al., 2000; Davison and Hwang, 2003; Ledzewicz and Schättler, 2007; Moonen, 2007). In one feedback-based therapy (Salomir et al., 2000), the heat source power was adjusted based on the deviation of temperature from a target at a particular location in the body, including an integral term, very similar to a PID controller. The desired response was that the temperature should rise quickly to the target without overshoot or oscillations.

Parker (2007) describes a strategy for "model-informed" treatment design for delivery of a chemotherapeutic agent. Using a combination of pharmacokinetic and pharmacodynamic models, predictions can be made about the patient's response (e.g., tumor volume) to the manipulated variables, which in this case could include the drug dosage level and schedule for drug administration. This strategy can be implemented by specifying the time horizon over which the patient's response is monitored and by calculating the optimal drug delivery protocol using the RTO methods of Chapter 19.

More recent developments include chemotherapy using antiangiogenic agents, which deprive the tumor from developing blood cells required for growth (Ledzewicz and Schättler, 2007). In this application, information about the state of the tumor (e.g., the tumor volume, derived from MRI data) is used to control the rate of dosing of the antiangiogenic therapy. More recently, model predictive control designs have been proposed for chemotherapeutic protocols, as an example of a decision support tool, as contrasted with an automation tool (Florian et al., 2008).

22.2.4 Controlled Treatment for HIV/AIDS

To address the global problem of HIV/AIDS, a number of mathematical models and control algorithms have been proposed to help design better treatments for the disease. The drug categories that have been considered include reverse transcriptase inhibitors and protease inhibitors, which affect reproduction of the virus via transcription and production of the virus from infected cells, respectively. The most effective strategies to date have involved a so-called cocktail of multiple drugs, thus attacking the disease in a vector direction (i.e., multiple, simultaneous targets). Measurements are problematic, consisting of relatively slow techniques based on off-line sampling of blood. However, the slow progression of the disease does not warrant real-time measurements, and thus feedback can still be accomplished on this slow time scale.

In their simplest form, mathematical models have been developed that describe the interactions of healthy CD4+ T cells, infected CD4+ T cells, and free viruses in the form of three coupled ordinary differential equations (Craig and Xia, 2005). Such a model can be the basis of simple model-based feedback strategies for control and can also be extended to generate more complex models suitable for a model predictive control strategy (Zurakowski et al., 2004).

22.2.5 Cardiac-Assist Devices

Cardiac-assist devices are mechanical pumps that provide cardiac output at an appropriate pressure, to allow normal circulation of blood through the patient's body, subject to the changing demands for cardiac output as a function of the patient's state (e.g., level of exercise, emotion, posture, etc.). The ideal device would mimic the body's own mechanisms for maintaining cardiac output at target levels; however, currently available devices are rather primitive in terms of automation, requiring the patient to adjust the set point (Boston et al., 2000). The first such implantable device received approval by the FDA over a decade ago.

One of the more interesting aspects of the control design problem for ventricular-assist devices is the placement of the sensors and actuators: there are the issues of susceptibility to infection, as well as anatomical placement (Paden et al., 2000).

22.2.6 Additional Medical Opportunities for Process Control

There are many other challenges in drug therapy, in which an optimized delivery regimen could be calculated using principles of process control and process optimization, e.g., the modeling and control of the anticoagulant drug, heparin (McAvoy, 2007). Another medical application is the treatment of acute neuropatients with brain hypothermia, to lower the intracranial pressure (ICP). A mathematical model can be developed to relate temperature effects with blood flow. The model can then be used to create an automated closed-loop controller (Gaohua and Kimura, 2006) to adjust the coolant temperature (e.g., by using cold-water circulating blankets) in an effort to regulate the ICP.

SUMMARY

Biological and biomedical processes share a great deal in common with the process applications considered in preceding chapters. The latter applications have a characteristic time constant, often exhibit time delays associated with measurements, and typically are multivariable in nature. In contrast, the types of uncertainties in bioprocesses are quite different, owing to the complex nature of biological regulation (see Chapter 23). In addition, there are multiple safety and regulatory issues that are unique to medical closed-loop systems. Process control strategies for several key unit operations in the bioprocess industries (fermentation, crystallization, and granulation) have been described, along with biomedical applications, such as drug delivery for diabetes and blood pressure control and other examples. In Chapter 23, we focus on the molecular scale of biological systems and consider the feedback mechanisms inherent in naturally occurring biophysical networks.

REFERENCES

Alford, J., Bioprocess Control: Advantages and Challenges, Proc. Conf. Chemical Process Control, Alberta (2006).

American Diabetes Association, Standards of Medical Care in Diabetes—2006, *Diabetes Care*, **29**, S4 (2006).

Araki, M., and E. Furutani, Computer Control of Physiological States of Patients under and after Surgical Operation Annu. Rev. Control, 29, 229 (2005).

Ashcroft, F. M., and S. J. H. Ashcroft, *Insulin: Molecular Biology to Pathology*, Oxford University Press, NY, 1992.

Bequette, B. W., *Process Control*, Prentice-Hall, Upper Saddle River, NJ, 2002.

Bequette, B. W., Modeling and Control of Drug Infusion in Critical Care, *J. Process Control*, **17**, 582 (2007).

Boston, J., M. Simaan, J. Antaki, and Y. Yu, Control Issues in Rotary Heart Assist Devices, *Proc. American Control Conference*, 3473 (2000).

Boudreau, M. A., and G. K. McMillan, New Directions in Bioprocess Modeling and Control, ISA, NC, 2007.

Buckland, B. C., The Translation of Scale in Fermentation Processes: The Impact of Computer Process Control, *Nature Biotechnology*, **2**, 875 (1984).

Craig, I., and X. Xia, Can HIV/AIDS Be Controlled?, *IEEE Control Sys.,* **25**, 80 (2005).

Davison, D. E., and E.-S. Hwang, Automating Radiotherapy Cancer Treatment: Use of Multirate Observer-Based Control, *Proc. American Control Conference*, 1194 (2003).

DCCT—The Diabetes Control and Complications Trial Research Group, The Effect of Intensive Treatment of Diabetes on the Development and Progression of Long-Term Complications in Insulin-Dependent Diabetes Mellitus, *New Engl. J. Med*., **329**, 977 (1993).

Dodd, G. D., M. C. Soulen, R. A. Kane, T. Livraghi, W. R. Lees, Y. Yamashita, A. R. Gillams, O. I. Karahan, and H. Rhim, Minimally Invasive Treatment of Malignant Hepatic Tumors: At the Threshold of a Major Breakthrough, *Radiographics*, **20**, 9 (2000).

Doyle, F., L. Jovanovič, D. Seborg, R. S. Parker, B. W. Bequette, A. M. Jeffrey, X. Xia, I. K. Craig, and T. J. McAvoy, A Tutorial of Biomedical Process Control, *J. Process Control*, **17**, 571 (2007).

Doyle, F., L. Jovanovič, and D. E. Seborg, Glucose Control Strategies for Treating Type 1 Diabetes Mellitus, *J. Process Control*, **17**, 572 (2007).

Fleet, G. H. (Ed.), *Wine Microbiology and Biotechnology*, Taylor & Francis, London, U.K., 1993.

Florian, J. A., J. L. Eiseman, and R. S. Parker. Nonlinear Model Predictive Control for Dosing Daily Anticancer Agents: A Tamoxifen Treatment of Breast Cancer Case Study, *Comput. Biol. Med*., **38**, 339 (2008).

Fujiwara, M., Z. K. Nagy, J. W. Chew, and R. D. Braatz, First-Principles and Direct Design Approaches for the Control of Pharmaceutical Crystallization, *J. Process Control*, **15**, 493 (2005).

Gaohua, L., and H. Kimura, A Mathematical Model of Intracranial Pressure Dynamics for Brain Hypothermia Treatment, *J. Theor. Biol*., **238**, 882 (2006).

Gatzke, E. P., and F. J. Doyle III, Model Predictive Control of a Granulation System Using Soft Output Constraints and Prioritized Control Objectives, *Powder Tech*., **121**, 149 (2001).

Hahn, J., T. Edison, and T. F. Edgar, Adaptive IMC Control for Drug Infusion for Biological Systems, *Control Eng. Practice*, **10**, 45 (2002).

Heller, A., Integrated Medical Feedback Systems for Drug Delivery, *AIChE J*., **51**, 1054 (2005).

Henson, M. A., and D. E. Seborg, An Internal Model Control Strategy for Nonlinear Systems, *AIChE J*., **37**, 1065 (1991).

Jovanovič, L., The Role of Continuous Glucose Monitoring in Gestational Diabetes Mellitus, *Diabetes Technol. Ther.*, **2**, S67 (2000).

Larsen, P. A., D. B. Patience, and J. B. Rawlings, Industrial Crystallization Process Control, *IEEE Control Systems*, **26**, 70 (2006).

Ledzewicz, U., and H. Schättler, Antiangiogenic Therapy in Cancer Treatment as an Optimal Control Problem, *SIAM J. Control Optim*., **46**, 1052 (2007).

Mahadevan, R., S. K. Agrawal, and F. J. Doyle III, Differential Flatness Based Nonlinear Predictive Control of Fed-Batch Bioreactors, *Control Eng. Prac*., **9**, 889 (2001).

Mandenius, C. -F., Process Control in the Bioindustry, *Chemistry Today*, 19 (1994).

McAvoy, T. J., Modeling and Control of the Anticoagulant Drug Heparin, *J. Process Control*, **17**, 590 (2007).

Moonen, C. T. W., Spatio-Temporal Control of Gene Expression and Cancer Treatment Using Magnetic Resonance Imaging-Guided Focused Ultrasound, *Clin. Cancer Res*., **13**, 3482 (2007).

Mort, P. R., S. W. Capeci, and J. W. Holder, Control of Agglomeration Attributes in a Continuous Binder-Agglomeration Process, *Powder Tech*., **117**, 173 (2001).

Paden, B., J. Ghosh, and J. Antaki, Control System Architectures for Mechanical Cardiac Assist Devices, *Proc. American Control Conference*, 3478 (2000).

Parker, R. S., Modeling for Anti-Cancer Chemotherapy Design, *J. Process Control*, **17**, 576 (2007).

Pottmann, M., B. A. Ogunnaike, A. A. Adetayo, and B. J. Ennis, Model-Based Control of a Granulation System, *Powder Tech*., **108**, 192 (2000).

Rao, R. R., J. W. Huang, B. W. Bequette, H. Kaufman, and R. J. Roy, Control of a Nonsquare Drug Infusion System: A Simulation Study, *Biotechnol. Prog*., **15**, 556 (1999).

Rohani, S., M. Haeri, and H. C. Wood, Modeling and Control of a Continuous Crystallization Process Part 1. Linear and Non-Linear Modeling, *Comput. Chem. Eng.*, **23**, 263 (1999).

Salomir, R., F. C. Vimeux, J. A. de Zwart, N. Grenier, and C. T. W. Moonen, Hyperthermia by MR-Guided Focused Ultrasound: Accurate Temperature Control Based on Fast MRI and a Physical Model of Local Energy Deposition and Heat Conduction, *Magnetic Resonance in Medicine*, **43**, 342 (2000).

Schügerl, K., Progress in Monitoring, Modeling and Control of Bioprocesses during the Last 20 Years, *J. Biotechnol.*, **85**, 149 (2001).

Steil, G. M., K. Rebrin, C. Darwin, F. Hariri, and M. F. Saad, Feasibility of Automating Insulin Delivery for the Treatment of Type 1 Diabetes, *Diabetes*, **55**, 3344 (2006).

Zisser, H., L. Jovanovič, F. Doyle III, P. Ospina, and C. Owens, Run-to-Run Control of Meal-Related Insulin Dosing, *Diabetes Technol. Ther.*, **7**, 48 (2005).

Zhou, G. X., M. Fujiwara, X. Y. Woo, E. Rusli, H. -H. Tung, C. Starbuck, O. Davidson, Z. Ge, and R. D. Braatz, Direct Design of Pharmaceutical Antisolvent Crystallization through Concentration Control, *Crystal Growth & Design*, **6**, 892 (2006).

Zurakowski, R., M. J. Messina, S. E. Tuna, and A. R. Teel, HIV Treatment Scheduling Via Robust Nonlinear Model Predictive Control, *Proc. Asian Control Conference*, 25 (2004).

EXERCISES

22.1 Consider the fermentor problem in Example 22.1.

(a) Design an IMC controller for the first operating point (dilution = .202 h^{-1}), and simulate the response to both a +0.5 [g/L] and a −0.5 [g/L] change in the biomass concentration set point. Then, simulate the response to both a +1 [g/L] and a −1 [g/L] change in the biomass concentration set point.

(b) Simulate the response of a −12.5% step change in the maximum growth rate (μ_m). How well does the controller perform?

(c) Comment on the observed nonlinearity in the system.

(d) Discuss how the controller design would change if there were a requirement to operate at the lower dilution operating point. What do you need to consider in this case?

22.2 Consider the granulation model that was given in Example 22.2.

(a) Design an MPC controller, using the nominal process model. Initially consider a control horizon of $M = 2$ and a prediction horizon of $P = 40$ (with a sampling period of $\Delta = 1$). Use equal weights on the manipulated inputs and penalize the two percentile outputs equally, but use a larger weight on the bulk density (y_1).

(b) Consider the effect of a plant-model mismatch. Use the problem statement for control design, but assume that the actual process is characterized by the following parameters:

$$\widehat{K}_{i,j} = \begin{bmatrix} 0.10 & 0.90 & 0.15 \\ 0.25 & 1.10 & 1.30 \\ 0.50 & 0.80 & 1.00 \end{bmatrix}$$

$$\widehat{\tau}_{i,j} = \begin{bmatrix} 1 & 2 & 1.5 \\ 3 & 3 & 3 \\ 3 & 3 & 3 \end{bmatrix}$$

$$\widehat{\theta}_{i,j} = \begin{bmatrix} 2 & 2 & 4 \\ 2 & 3 & 4 \\ 2 & 3 & 4 \end{bmatrix}$$

(c) These models are in deviation variables, but the actual steady-state flow rates for the nozzles are 175, 175, and 245, respectively. The steady-state outputs are 40, 400, and 1,620, respectively. Nozzle flow rates are limited to values between 100 and 340, and it is desired to keep the 5th percentile (y_2) above 350 and the 90th percentile (y_3) below 1,650. Simulate the response of the controller to the following changes:

- **(i)** Step change in bulk density from 40 to 90.
- **(ii)** Simultaneous change in the 5th percentile from 400 to 375 and 90th percentile from 1,620 to 1,630.

Comment on the performance of your controller (and retune as necessary).

22.3 Gaohua and Kimura (2006) derived an empirical patient model for the manipulation of ambient temperature u (°C) to influence the patient's brain intracranial pressure (ICP) y (mm Hg). The medical data support the following empirical values for a first-order-plus-time-delay model to describe the effect of cooling temperature (°C) on the ICP (mmHg) in time units of hours:

$$G(s) = \frac{4.7}{9.6s + 1} e^{-s}$$

The nominal values for the process variables are: ICP = 20 mmHg; ambient temperature = 30°C.

(a) Using the IMC tuning rules, derive an appropriate PI controller for this medical experiment. (*Hint:* begin with a value $\tau_c = 1.0$ [h]). What does that value of τ_c mean?

(b) Simulate the response of a 10-mmHg reduction in ICP. What is the overshoot? What is the minimum value of the temperature? What is the settling time?

(c) Comment on whether this is a reasonable controller design for a biomedical application. How might you improve the design?

22.4 In a rehabilitation training experiment for a neurological patient, a step change in treadmill speed of +2.5 km/h was made. The patient heart rate response HR is given in Figure E22.4.

(a) Derive an appropriate first-order-plus-time-delay model for the patient dynamics.

(b) The doctors wish to control the patient's heart rate to a nearly constant value by adjusting treadmill speed. Using the IMC tuning rules, design a suitable PI controller for this patient. Simulate the response of the controller for a step change in the HR of +10 bpm. Calculate the settling time, overshoot, and rise time for the controller. Do these values seem reasonable for a medical application?

(c) How would you improve the procedure for fitting the patient's initial dynamics?

22.5 A crystallizer is used to separate a pharmaceutical product from the fermentation extract. The three manipulated variables are the fines dissolution rate (u_1), the crystallizer temperature (u_2), and the flow rate in the overflow (u_3). The nominal values of these three inputs are 2.25×10^{-6} m^3/s, 310 K, and 1.5×10^{-6} m^3/s, respectively. The three variables to be controlled are the crystal size distribution, as calculated by the fines suspension density (y_1); the crystal purity, as

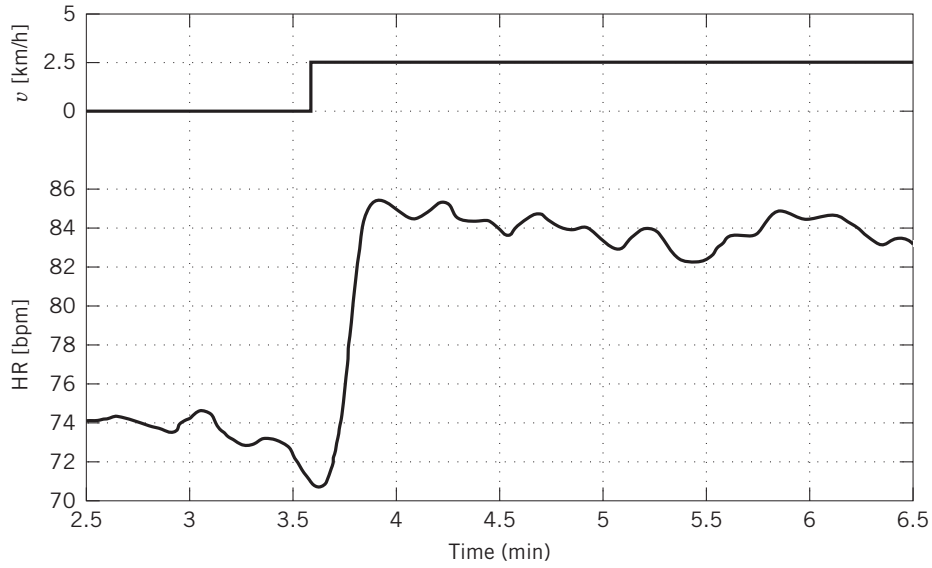

Figure E22.4

calculated by supersaturation conditions (y_2); and the product rate (y_3). The nominal values of these three inputs are 0.55 K, 11.23 K, and 0.12 kg/kg H_2O, respectively. These variables have multiple interactions, and the following model has been identified from experimental data for a continuous crystallizer, where time is measured in s (Rohani et al., 1999):

$$\begin{bmatrix} y_1 \\ y_2 \\ y_3 \end{bmatrix} = \begin{bmatrix} \dfrac{72{,}600}{s+0.2692} & \dfrac{0.025082(s-20.0)(s-10.4)}{s^2+10.11s+96.57} & \dfrac{125{,}000(s-1.25)}{s+0.39} \\ \dfrac{568{,}000}{s+2.11} & \dfrac{-0.15095}{s+0.1338} & \dfrac{-1{,}830{,}000(s+0.089)}{s+0.43} \\ \dfrac{-1{,}870}{s+0.21} & \dfrac{-0.0071}{s+0.235} & \dfrac{16{,}875}{s+0.2696} \end{bmatrix} \times \begin{bmatrix} u_1 \\ u_2 \\ u_3 \end{bmatrix}$$

(a) Calculate the RGA, and determine the appropriate pairings for SISO feedback control. Comment on the role of dynamics in your decision.

(b) Using the IMC tuning rules, design three PI controllers for this process.

(c) Simulate the process response to a step set point, separately, in each of the controlled outputs [use a magnitude of +10% (relative) change]. Next, simulate the response of the system to a simultaneous pair of step changes (again, use a magnitude of +10% relative) in each of the second (purity) and third (product rate) controlled outputs. Try to tune the controller to improve the transient response to the simultaneous step changes.

22.6 Consider the diabetic patient in Example 22.3. Your goal is to design an automated device to administer insulin infusion in response to meal disturbances.

(a) Considering only the insulin-glucose dynamics, calculate an approximate second-order patient model by fitting the responses (changes in insulin) obtained from simulations of the equations given in the example.

(b) Using the IMC tuning rules, design a PID controller for this process.

(c) Simulate the closed-loop system response to a step set-point change in blood glucose of –20 mg/dl. Try to tune the controller to improve the transient response.

(d) Simulate the closed-loop system response to the meal disturbance described in Example 22.4. Is the controller able to maintain the safety boundaries for blood glucose (54 mg/dL $<$ G $<$ 144 mg/dL)?

(e) In practice, the sensors are available for measuring blood glucose sample from the subcutaneous tissue (the layer of fat under the skin, as opposed to directly from the blood stream). Assuming that such a procedure introduces a pure delay, repeat the simulation from part (d) with a 10-min sensor delay. How has the performance changed? What is the maximum time delay that the closed-loop design will tolerate before it becomes unstable?